

Research Article

Power-Controlled CDMA Cell Sectorization with Multiuser Detection: A Comprehensive Analysis on Uplink and Downlink

Changyoon Oh and Aylin Yener

Electrical Engineering Department, The Pennsylvania State University, PA 16802, USA

Received 8 November 2006; Revised 14 July 2007; Accepted 12 October 2007

Recommended by Hyung-Myung Kim

We consider the joint optimization problem of cell sectorization, transmit power control and multiuser detection for a CDMA cell. Given the number of sectors and user locations, the cell is appropriately sectorized such that the total transmit power, as well as the receiver filters, is optimized. We formulate the corresponding joint optimization problems for both the uplink and the downlink and observe that in general, the resulting optimum transmit and receive beamwidth values for the directional antennas at the base station are different. We present the optimum solution under a general setting with arbitrary signature sets, multipath channels, realistic directional antenna responses and identify its complexity. We propose a low-complexity sectorization algorithm that performs near optimum and compare its performance with that of optimum solution. The results suggest that by intelligently combining adaptive cell sectorization, power control, and linear multiuser detection, we are able to increase the user capacity of the cell. Numerical results also indicate robustness of optimum sectorization against Gaussian channel estimation error.

Copyright © 2007 C. Oh and A. Yener. This is an open access article distributed under the Creative Commons Attribution License, which permits unrestricted use, distribution, and reproduction in any medium, provided the original work is properly cited.

1. INTRODUCTION

Future wireless systems are expected to provide high-capacity flexible services. Code division multiple access (CDMA) shows promise in meeting the demand for future wireless services [1]. It is well known that CDMA systems are interference-limited and the capacity of CDMA systems can be improved by various interference management techniques. These techniques include transmit power control where transmit power levels are adjusted to control interference, multiuser detection where receiver filters are designed to separate interfering signals, and beamforming and cell sectorization where arrays and directional antennas are utilized to suppress interference [2–10]. While earlier work on interference management techniques proposed the aforementioned methods as alternatives to each other, more recent research efforts recognized the capacity improvement by employing these techniques jointly. To that end, jointly optimum transmit power control and receiver design, jointly optimum transmit power control and cell sectorization, and jointly transmit power control, beamformer, and receiver filter design have been considered in [2, 3, 7].

Jointly combining beamformer and receiver filter along with transmit power control improves the system performance. However, using beamforming requires intensive

feedback to guarantee its performance. Hence, using sectorized antenna could be a good alternative low-cost option. In this paper, we consider a CDMA system where the base station is equipped with directional antennas with variable beamwidth [11] and investigate the joint optimization problem of cell sectorization, power control, and multiuser detection. Given the number of sectors and terminal locations and the fact that the base station (for uplink) and the terminals (for downlink) employ linear multiuser detection, the problem we consider is to appropriately sectorize the cell, that is, to determine the main beamwidth of the directional antennas to be used at the base station, such that the total transmit power is minimized, while each terminal has an acceptable quality of service. The quality of service (QoS) measure we adopt is the signal-to-interference ratio (SIR). In the sequel, we use the terms “terminal” and “user” interchangeably.

Conventional cell sectorization, where the cell is sectorized to equal angular regions, may not perform sufficiently well especially in systems where user distribution is nonuniform [2]. Previous work has shown that *adaptive cell sectorization* where sector boundaries are adjusted in response to terminal locations greatly improves the uplink user capacity [2]. Preliminary results also indicate that uplink capacity can be further improved when adaptive cell sectorization is employed in conjunction with linear multiuser detection [12].

Adaptive cell sectorization [2, 12–15] can be interpreted as dynamically grouping users in the pool of spatial orthogonal channels provided by perfect directional antennas. In the special case, when the system employs random signatures or a deterministic equicorrelated signature set, the minimum received power in each sector is achieved when all users' received powers are equal, and there exists a closed-form solution for the optimum received power in each sector. In this case, the transmit power optimization problem can be transformed into a graph partitioning problem whose solution complexity is polynomial in the number of users and sectors. Works in [2, 12] considered such special cases when matched filters and linear multiuser detectors are employed at the base station. Both [2, 12] also assumed perfect directional antenna response, that is, complete orthogonality between sectors. We also note that, for improvement of the downlink user capacity, heuristic methods to adjust sector boundaries have been reported previously (e.g., see [13]).

In general, it is more reasonable to assume that users (for uplink) and the base station (for downlink) experience a frequency-selective channel in which it becomes difficult to justify the equicorrelated signature assumption in [2]. In addition, it is not possible to expect the directional antenna to completely filter out all transmissions/receptions outside its main beamwidth. This fact leads to intersector interference (ISecI) and, as we observe in the sequel, alters the optimum sectorization arrangement found in [2].

The preceding discussion suggests that, while previous work [2, 12–15] has paved the way for demonstrating the benefits of adapting the size of each sector to improve user capacity, a comprehensive mathematical analysis of more practical scenarios, where the limiting system model assumptions are relaxed, is needed to demonstrate the real value of adaptive cell sectorization both for the uplink and the downlink. This paper aims to provide this analysis and answer the question of how to adjust the sector boundaries to optimize the user capacity using transmit power control and receiver filter design. We consider both the uplink and the downlink problems and observe that the two problems in general do not lead to identical sectorization arrangements. We examine the optimum solution in each case and propose near-optimum methods with reduced complexity. Our numerical results suggest that the uplink/downlink user capacity in realistic scenarios significantly benefits from intelligently combining cell sectorization, power control, and receiver filtering. Lastly, our numerical results also consider the effect of channel estimation errors on adaptive sectorization. We observe that adaptive sectorization is robust against users' channel estimation errors; that is, slightly increased user transmit power can compensate for user's channel estimation errors, while optimum sectorization arrangement remains the same.

2. ANTENNA PATTERN AND SYSTEM MODEL

2.1. Antenna pattern

Following [11, 16], we use the antenna pattern shown in Figure 1 for transmission and reception at the base sta-

tion.¹ Due to the existence of side lobes in the antenna pattern, interference (ISecI) results from adjacent sectors. Main lobe between θ_1 and $-\theta_1$ (within the sector) has a constant antenna gain, 0 dB, and the side lobes between θ_1 and θ_2 and $-\theta_2$ and $-\theta_1$ (out of sector) have linear attenuated antenna gain in dB. The other angular area has a flat antenna gain, P dB. The larger $\delta = \theta_2 - \theta_1$ is, the larger the area spanned by the sector antenna will be, which causes increased ISecI. Typically, δ is small compared to the size of the main lobe, but it is nonnegligible. Uplink and downlink ISecI patterns are in general quite different as explained in what follows.

2.1.1. Uplink ISecI pattern

All users within a sector between θ_1 and $-\theta_1$ experience interference from the same set of out-of-sector users. Thus, the amount of ISecI at the *front end* of the receiver filters for all users in the sector is the same. The base station receives all in-sector users' signals (users whose angular locations lie between θ_1 and $-\theta_1$) with unity antenna gain and all out-of-sector users' signals (users whose angular locations lie outside θ_1 and $-\theta_1$) with attenuated antenna gain following the pattern in Figure 1. Especially, side lobe gains between θ_1 and θ_2 and between $-\theta_1$ and $-\theta_2$ cause major ISecI.

2.1.2. Downlink ISecI pattern

The base station transmits users' signals through their assigned sector antennas as in Figure 1(b). When we look at a given sector area, we see that each user experiences a different level of ISecI depending on the user's angular location. Users between θ_3 and θ_4 experience no major ISecI, because the side lobes of the adjacent sector antennas do not reach that region between θ_3 and θ_4 . On the other hand, users between $-\theta_1$ and θ_3 , θ_4 , and θ_1 do experience major ISecI. The level of ISecI these users experience depends on the side lobe antenna gain of the adjacent sectors. Clearly, users closer to the boundaries, $-\theta_1$ or θ_1 , will experience more ISecI. Users whose angular locations lie in all neighbor sectors, that is, sectors whose antenna reaches that region between $-\theta_1$ and θ_3 and θ_4 and θ_1 , contribute to the ISecI.

Note that the uplink sidelobe antenna gain, which is from out-of-sector interferer to user i , v_{li}^{up} is a function of the angular location of out-of-sector interferer l . On the other hand, the downlink sidelobe antenna gain, which is from out-of-sector interferer to user i , v_{li}^{down} is a function of the angular location of user i . Consequently, v_{li}^{up} is different from v_{li}^{down} in general.

¹ The aim in this paper is to adjust the antenna beamwidth, for a given antenna beam pattern, to include the number of users in each sector with the consideration of imperfect antenna pattern. Joint optimization of transmit power control, beamforming, and receiver filter design has been investigated in [3].

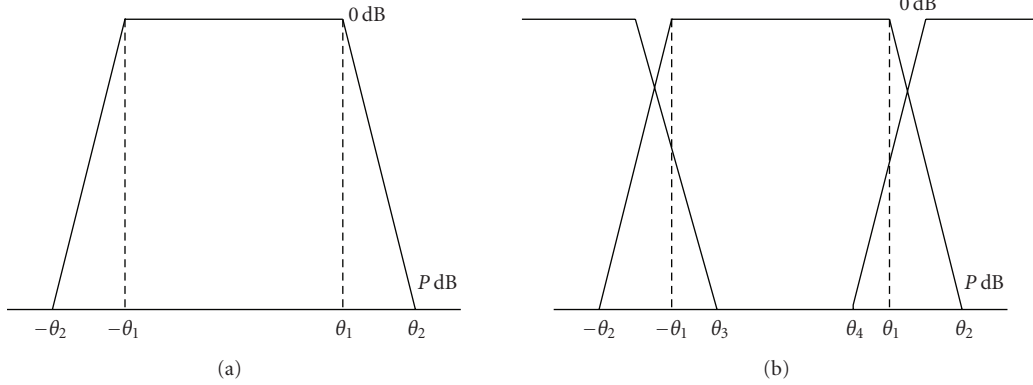


FIGURE 1: (a) Uplink/downlink antenna pattern model and (b) intersector interference model.

2.2. System model

A DS-CDMA cell with processing gain N and M users is considered. The locations and the channels of the users in the cell are assumed to be known at the base station and will not change in respect of the duration of interest. This is a reasonable assumption in a slow mobility environment or in fixed wireless systems. Our formulation will assume perfect channel knowledge. In the numerical results, we show the robustness of cell sectorization in the presence of channel estimation errors. We assume that the cell is to be sectorized to K sectors.

2.2.1. Uplink

Signature of user i , s_i^* , goes through the multipath channel \mathbf{G}_i , which is an $N \times N$ lower triangular matrix for user i whose (a, b) th entry $G_i(a, b)$ represents $(a - b)$ th multipath gain.² N is equal to the length of signature sequence. We define the path-loss-based channel gain for user i , and we define h_i as a separate quantity; that is, the overall channel response is a scalar multiple of \mathbf{G}_i . This model assumes that the multiple paths are chip synchronized, and the j th path represents the copy that arrives at the receiver with a delay of j chips. We consider the bit duration as our observation interval. We assume the symbol synchronous model and the fact that the number of resolvable paths is less than the processing gain.³ Accordingly, the resulting intersymbol interference can be negligible. Thus, we ignore intersymbol interference for clarity of exposition. Let the signature of user i after going through the multipath channel of user i be $\mathbf{s}_i = \mathbf{G}_i \mathbf{s}_i^*$.

After chip-matched filtering and sampling, the received signal vector for user i at the base station is

$$\mathbf{r}_i = \sqrt{p_i} h_i \mathbf{b}_i \mathbf{s}_i + \sum_{j \neq i, j \in g_k(\theta)} \sqrt{p_j} h_j \mathbf{b}_j \mathbf{s}_j + \sum_{l \notin g_k(\theta)} \sqrt{p_l} h_l v_{li} \mathbf{b}_l \mathbf{s}_l + \mathbf{n}, \quad (1)$$

where p_i , h_i , \mathbf{b}_i are the transmit power, the channel gain, and the information bit for user i . \mathbf{s}_i is the signature sequence of length N for user i . \mathbf{n} denotes the zero-mean Gaussian noise vector with $E(\mathbf{n}\mathbf{n}^\top) = \sigma^2 \mathbf{I}_N$. θ is the N -tuple vector whose j th component denotes the main beamwidth for sector j in radians. $g_k(\theta)$ ($k = 1, \dots, K$) is the set of users that resides in the area spanned by sector k . The second term in (1) represents the intrasector interference, while the third term represents the ISeI. v_{li} is antenna gain between interferer l and user i . It is important to note that $v_{li} \neq v_{il}$; that is, the cause of the two mutually interference out-of-sector terminals for each other may be different, depending on the antenna pattern and the users' locations. In particular, user l may lie within the receive range of the antenna serving the sector where user i resides, hence contributing to the ISeI for user i , while user i may reside outside the range of the receive antenna of the sector in which user l resides, without contributing to the ISeI for user l .

2.2.2. Downlink

Following [17], the transmitted signal vector⁴ from the sector antenna k can be expressed as

$$\mathbf{x} = \sum_{j \in g_k(\theta)} \sqrt{p_j} \mathbf{b}_j \mathbf{s}_j, \quad k = 1, \dots, K, \quad (2)$$

² Note that in the uplink, s_i^* denotes the signature of user i for clarity of exposition, while s_i is used for signature of user i in the downlink.

³ With the assumption that the number of resolvable paths is less than the processing gain N with no intersymbol interference, multipath channel matrix with size $N \times N$ is enough to represent the multipath channel.

⁴ Typically in the downlink, orthogonal sequences are used, while random sequences are used in the uplink. However, due to multipath channel, the orthogonality in the downlink would be typically lost at the receiver side leading to interference.

where p_j and \mathbf{s}_j are the transmit power and the signature sequence the base station uses to transmit b_j to user j .

User i receives \mathbf{r}_i through the multipath channel \mathbf{G}_i . Let the signature of user j after going through the multipath channel of user i be $\mathbf{s}_j^i = \mathbf{G}_i \mathbf{s}_j$. Then, following the description of our model, the received signal for user i is given by

$$\mathbf{y}_i = \sqrt{p_i} h_i b_i \mathbf{s}_i^i + \sum_{j \neq i, j \in g_k(\underline{\theta})} \sqrt{p_j} h_i b_j \mathbf{s}_j^i + \sum_{l \notin g_k(\underline{\theta})} \sqrt{p_l} h_i v_{li} b_l \mathbf{s}_l^i + \mathbf{n}_i, \quad (3)$$

where \mathbf{n}_i is the white Gaussian noise vector. Once again, v_{li} is the antenna gain between interferer l and user i , and $v_{li} \neq v_{il}$ (see Figure 1).

3. PROBLEM FORMULATION

Our aim in this paper is to improve the user capacity of the CDMA cell, that is, increasing the number of simultaneous users that achieves their quality of service requirements. This will be accomplished by employing jointly optimal power control and multiuser detection, and by designing variable width sectors that lead to the assignment of each user to its corresponding directional antenna. We consider the user capacity enhancement problem for both the uplink and the downlink. In each case, our metric is the transmit power expended in the cell, while guaranteeing each user with its minimum quality of service. A user is said to have an acceptable quality of service if its SIR is greater than or equal to a target SIR, γ^* . In the uplink, the minimum total transmit power minimization problem has the additional advantage of battery conservation for each user. In the downlink, the problem can be interpreted as one that yields strategies that can accommodate more simultaneous users for a given transmit power at the base station. In each case, we need to find non-negative power values and design the sectors such that the entire cell is covered. The corresponding transmit power optimization problem is given by

$$\begin{aligned} \min_{\underline{\theta}, \mathbf{p}, \mathbf{c}} \quad & \sum_{k=1}^K \sum_{i \in g_k(\underline{\theta})} p_i \\ \text{s.t.} \quad & \text{SIR}_i = \frac{P_{i,S}}{P_{i,\text{INTRA}} + P_{i,\text{INTER}} + P_{i,\text{NOISE}}} \geq \gamma^*, \\ & i = 1, \dots, M, \quad \mathbf{p} \geq \mathbf{0}, \quad \mathbf{1}^\top \underline{\theta} = 2\pi, \end{aligned} \quad (4)$$

where $P_{i,S}$, $P_{i,\text{INTRA}}$, $P_{i,\text{INTER}}$, and $P_{i,\text{NOISE}}$ represent the desired signal power, intrasector interference power, intersector interference power, and the noise power, experienced by user i , respectively. $\underline{\theta}$, \mathbf{p} , $\mathbf{c} = \{\mathbf{c}_1, \dots, \mathbf{c}_M\}$ are set of sector arrangements, power vector for all users in the cell, receiver filter set for all users, respectively. Each of these terms will vary for uplink and downlink leading to the corresponding SIR expressions. In addition, the SIR is a function of the transmit powers and receiver filters over which we will conduct optimization. A moments thought reveals that the receiver filter of user i affects the SIR of user i only, and similar to the single-

sector joint power control and multiuser detection [7], the filter optimization can be moved to the SIR constraint:

$$\begin{aligned} \min_{\underline{\theta}, \mathbf{p}} \quad & \sum_{k=1}^K \sum_{i \in g_k(\underline{\theta})} p_i \\ \text{s.t.} \quad & \max_{\mathbf{c}_i} \text{SIR}_i \geq \gamma^*, \quad i = 1, \dots, M, \\ & \mathbf{p} \geq \mathbf{0}, \quad \mathbf{1}^\top \underline{\theta} = 2\pi. \end{aligned} \quad (5)$$

For the uplink, the terms that contribute to the SIR expression for user i are found by filtering \mathbf{r}_i in (1) using the receiver filter of user i , \mathbf{c}_i , leading to

$$\begin{aligned} P_{i,S} &= p_i h_i (\mathbf{c}_i^\top \mathbf{s}_i)^2, & P_{i,\text{INTRA}} &= \sum_{j \neq i, j \in g_k(\underline{\theta})} p_j h_j (\mathbf{c}_i^\top \mathbf{s}_j)^2, \\ P_{i,\text{INTRA}} &= \sum_{l \notin g_k(\underline{\theta})} p_l h_l v_{li} (\mathbf{c}_i^\top \mathbf{s}_l)^2, & P_{i,\text{NOISE}} &= \sigma^2 (\mathbf{c}_i^\top \mathbf{c}_i). \end{aligned} \quad (6)$$

The transmit power optimization problem for the uplink (UTP) entails finding radial value of each directional antenna beamwidth, the transmit power of each user, and the linear receiver filter for each user at the base station, in a jointly optimum fashion. It is straightforward to see that, in this case, (5) becomes

$$\begin{aligned} \min_{\underline{\theta}, \mathbf{p}} \quad & \sum_{k=1}^K \sum_{i \in g_k(\underline{\theta})} p_i \quad (\text{UTP}) \\ \text{s.t.} \quad & p_i \geq \min_{\mathbf{c}_i} \frac{\gamma^* (D_1 + D_2 + \sigma^2 (\mathbf{c}_i^\top \mathbf{c}_i))}{h_i (\mathbf{c}_i^\top \mathbf{s}_i)^2}, \quad \mathbf{p} \geq \mathbf{0}, \quad \mathbf{1}^\top \underline{\theta} = 2\pi, \end{aligned} \quad (7)$$

where,

$$\begin{aligned} D_1 &= \sum_{j \neq i, j \in g_k(\underline{\theta})} p_j h_j (\mathbf{c}_i^\top \mathbf{s}_j)^2, \\ D_2 &= \sum_{l \notin g_k(\underline{\theta})} p_l h_l v_{li} (\mathbf{c}_i^\top \mathbf{s}_l)^2. \end{aligned} \quad (8)$$

For the downlink, the SIR for user i residing in sector k is found by filtering \mathbf{y}_i in (3), with user i 's receiver filter, \mathbf{c}_i , and it includes contributions from intra- and intersector interferences that arise from the base station's transmission to other users going through the multipath channel of user i as described in Section 2.2. This leads to

$$\begin{aligned} P_{i,S} &= p_i h_i (\mathbf{c}_i^\top \mathbf{s}_i)^2, & P_{i,\text{INTRA}} &= \sum_{j \neq i, j \in g_k(\underline{\theta})} p_j h_j (\mathbf{c}_i^\top \mathbf{s}_j)^2, \\ P_{i,\text{INTRA}} &= \sum_{l \notin g_k(\underline{\theta})} p_l h_l v_{li} (\mathbf{c}_i^\top \mathbf{s}_l)^2, & P_{i,\text{NOISE}} &= \sigma^2 (\mathbf{c}_i^\top \mathbf{c}_i). \end{aligned} \quad (9)$$

The downlink transmit power (DTP) optimization problem becomes

$$\begin{aligned} \min_{\underline{\theta}, \mathbf{p}} \quad & \sum_{k=1}^K \sum_{i \in g_k(\underline{\theta})} p_i \quad (\text{DTP}) \\ \text{s.t.} \quad & p_i \geq \min_{\mathbf{c}_i} \frac{\gamma^* (D_3 + D_4 + \sigma^2 (\mathbf{c}_i^\top \mathbf{c}_i))}{h_i (\mathbf{c}_i^\top \mathbf{s}_i)^2}, \quad \mathbf{p} \geq \mathbf{0}, \quad \mathbf{1}^\top \underline{\theta} = 2\pi, \end{aligned} \quad (10)$$

where

$$\begin{aligned} D_3 &= \sum_{j \neq i, j \in g_k(\theta)} p_j h_i (\mathbf{c}_i^\top \mathbf{s}_j^i)^2, \\ D_4 &= \sum_{l \notin g_k(\theta)} p_l h_i v_{li} (\mathbf{c}_i^\top \mathbf{s}_l^i)^2, \end{aligned} \quad (11)$$

p_i represents the power transmitted by the base station to communicate to user i , and the cost function in (10) is the total power transmitted by the base station.

4. UPLINK AND DOWNLINK SECTORIZATIONS

Given the problem formulations in the previous section, a valid question is to ask whether the optimum sectorization arrangement would be identical both from the uplink and downlink perspectives.

At the outset, by comparing UTP and DTP, one might believe that the optimum solutions should be identical. However, a closer look reveals that such a statement can be made only under a specific set of conditions. In particular, for a cellular system with no sectorization, it is well known that if the base station for each user to maintain an acceptable level of SIR is fixed and given, under the assumption of identical channel gains for uplink and downlink between each user and base station, the condition for feasibility of the uplink and the downlink power control problems is the same [18, 19]. Further, the work in [19] shows that in this case the optimum total transmit power of all users (uplink) is identical to the optimum total transmit power of all base stations (downlink).

Let us consider a similar scenario for the system model we have at hand. Consider the case where there is no ISeCI; that is, each sector is perfectly isolated. Assume that matched filter receivers are used; that is, no receiver filter optimization is done. We note that this scenario, in the uplink, is a slightly more general model than that of [2], in which we assume arbitrarily correlated sequences as opposed to pseudorandom sequences. Also, assume that the signature sequence for each user is identical to the downlink signature used to transmit to this user from a single-path channel. Uplink and downlink channel gains between a user and the base station and noise power values at all receivers are also identical. We will call this setting a ‘‘symmetric system.’’ Note that in this case, the UTP and DTP become

$$\begin{aligned} \min_{\theta, \mathbf{p}} \quad & \sum_{k=1}^K \sum_{i \in g_k(\theta)} p_i \\ \text{s.t.} \quad & \frac{p_i h_i}{\sum_{j \neq i, j \in g_k(\theta)} p_j h_j (\mathbf{s}_i^\top \mathbf{s}_j)^2 + \sigma^2} \geq \gamma^*, \quad i = 1, \dots, M, \end{aligned} \quad (12)$$

$$\begin{aligned} \min_{\theta, \mathbf{p}} \quad & \sum_{k=1}^K \sum_{i \in g_k(\theta)} q_i \\ \text{s.t.} \quad & \frac{q_i h_i}{\sum_{j \neq i, j \in g_k(\theta)} q_j h_j (\mathbf{s}_i^\top \mathbf{s}_j)^2 + \sigma^2} \geq \gamma^*, \quad i = 1, \dots, M, \end{aligned} \quad (13)$$

where we denoted the downlink power used to transmit to user i as q_i to distinguish it from the uplink power that user i transmits with p_i . Noting that the minimum transmit power is achieved when the SIR constraints are satisfied with equality [9, 17], we first make the following observation.

Observation 1. *For the symmetric system, under a given sectorization arrangement, the minimum total sector transmit powers for uplink/downlink are equal.*

Proof. The proof of this observation is straight forward using simple linear algebra and it is given in the appendix.⁵ \square

An immediate corollary of the above observation is that the total *cell transmit powers* for uplink and downlink are equal for any given sectorization arrangement. We can now make the following observation.

Observation 2. *If under a given sectorization arrangement the minimum total transmit powers for uplink and downlink are identical, then the optimum sectorization arrangements in terms of minimum transmit powers for uplink and downlink are also identical.*

Proof. Assume that the observation is false. Let $\{g_k(\theta_1)\}_{k=1, \dots, K}$ be optimum uplink sectorization arrangement and $\{g_k(\theta_2)\}_{k=1, \dots, K}$, where $\theta_2 \neq \theta_1$ is the optimum downlink sectorization arrangement. Since the cell total transmit powers for uplink and downlink are identical, we have

$$\sum_{k=1}^K \sum_{i \in g_k(\theta_1)} p_i = \sum_{k=1}^K \sum_{i \in g_k(\theta_1)} q_i > \sum_{k=1}^K \sum_{i \in g_k(\theta_2)} q_i = \sum_{k=1}^K \sum_{i \in g_k(\theta_2)} p_i, \quad (14)$$

which implies that $\{g_k(\theta_1)\}_{k=1, \dots, K}$ cannot be optimum uplink sectorization arrangement. Therefore, we have shown by contradiction that the uplink and downlink optimum sectorization arrangements have to be identical. \square

We note that Observation 2 is independent of the symmetry assumptions and a general statement. However, for the statement to be true, we need the equivalence of the uplink and downlink total transmit power values. The symmetric system is one for which this is guaranteed, and consequently we can easily claim that the converse of Observation 2 is also true.

We have seen that, under a set of system assumptions, we can hope to have the same optimum sectorization arrangement for the uplink and downlink. Such a scenario would simplify the calculation of the optimum transmit powers for the downlink once the uplink sectorization problem is solved. Unfortunately, once we introduce the receiver filter optimization to the problem, that is, as in UTP (7) and DTP

⁵ Note that the proof here is different from that in [19] in which we consider the case of arbitrary signature sequences.

(10), we can no longer guarantee the validity of Observation 1 even under reciprocal channel gains and signature sequences. The reason for this is that the resulting receiver filters are a function of the received power values [7]. In addition, in cases where we must take into account the intersector interference, as explained in Section 2.2, the fact that the ISecl one user causes to another user is not reciprocal, that is, $v_{ij} \neq v_{ji}$, and the fact that $v_{li}^{\text{up}} \neq v_{li}^{\text{down}}$ prevent us from claiming that the sectorization arrangement would be identical in general. Hence, we conclude that in general each direction should be optimized separately, by solving UTP and DTP. In Section 7, we will see by an example that the resulting sectorization arrangements in each direction are different.

5. OPTIMUM SECTORIZATION

The previous sections have formulated UTP and DTP and argued that in the most general formulation, they each lead to different sectorization arrangements. In this section, we will describe how to obtain the optimum solution.

We first note that, unlike the case where each sector is perfectly isolated, that is, the no ISecl case, we cannot consider each sector independently and that we need to run “cell-wide” power control. We also note that due to the lack of symmetry of antenna gains, that is, $v_{ij} \neq v_{ji}$, and the fact that they depend on the membership in a sector, integrated base station assignment and power control algorithms in [20] cannot be directly applied. Furthermore, although for each sectorization pattern there is an iterative algorithm that guarantees convergence to the optimum powers and receiver filters, as will be described shortly, there is no simple algorithm to choose the best sectorization arrangement. Hence, to find the jointly optimum sectorization arrangement, receiver filters, and transmit powers for all users in the cell, we need to consider all sectorization arrangements for which the corresponding grouping of users yields a feasible power control problem.

We note that the difference of the sectorization problem, from the channel allocation-/scheduling-type problems that have exponential complexity in the number of users [21], is the fact that in the sectorization problem the number of possible groupings of users is limited due to the physical constraints, that is, their angular positions in the cell. Similar to [2], we can represent the system by a graph, that is, a ring where each user’s angular position in the cell is mapped to the same angular position on the ring (see Figure 2). It is easy to see that the number of all possible sectorization arrangements is $\binom{M}{K}$.

For each feasible sectorization arrangement, an iterative algorithm that finds the minimum power solution along with the best linear filters is easily obtained as outlined below.

Consider the minimum total power solution, given a feasible sectorization arrangement. Define the power vector for all users in the cell as $\mathbf{p} = [p_1, \dots, p_{M_1}, p_1, \dots, p_{M_2}, \dots, p_1, \dots, p_{M_K}]^T$, where M_i is number of users in the

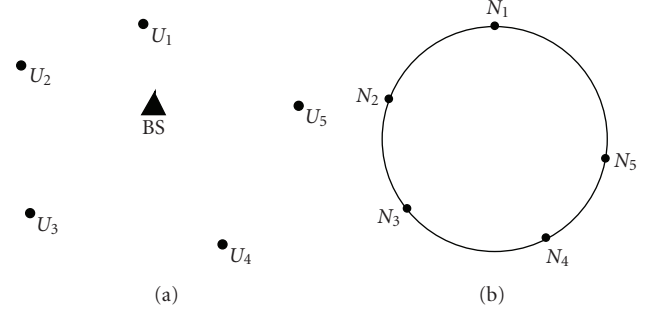


FIGURE 2: (a) User locations in a cell and (b) ring network constructed from the user locations. Node N_i in the ring corresponds to user U_i .

sector i and

$$I_{ki}(\mathbf{p}, \mathbf{c}_i) = \frac{\gamma^* (P_{i,\text{INTRA}} + P_{i,\text{INTER}} + P_{i,\text{NOISE}})}{h_i(\mathbf{c}_i^T \mathbf{s}_i)^2} \quad (\text{IF-UTP}) \quad (15)$$

for the uplink, and

$$I_{ki}(\mathbf{p}, \mathbf{c}_i) = \frac{\gamma^* (P_{i,\text{INTRA}} + P_{i,\text{INTER}} + P_{i,\text{NOISE}})}{h_i(\mathbf{c}_i^T \mathbf{G}_i \mathbf{s}_i)^2} \quad (\text{IF-DTP}) \quad (16)$$

for the downlink. We define the interference function $I(\mathbf{p})$ which is optimized by receiver filter as

$$I_{ki}(\mathbf{p}) = \min_{\mathbf{c}_i} I_{ki}(\mathbf{p}, \mathbf{c}_i), \quad (17)$$

$$\mathbf{I}(\mathbf{p}) = [I_{11}(\mathbf{p}), \dots, I_{1M_1}(\mathbf{p}), \dots, I_{21}(\mathbf{p}), \dots, I_{KM_K}(\mathbf{p})]. \quad (18)$$

The work in [9] showed that power control algorithms in the form of $\mathbf{p}(n+1) = \mathbf{I}(\mathbf{p}(n))$ converge to the minimum power solution if $\mathbf{I}(\mathbf{p})$ is a standard interference function. The proof that (18) is a standard interference function follows directly from the proof given in [7] for single-sector systems. The resulting power control algorithm first finds the receiver filter for user i to be the MMSE filter for fixed power vectors:

$$\begin{aligned} (\text{U-PC}) \quad \mathbf{A}_{ki}(\mathbf{p}(n)) &= \sum_{j \neq i, j \in g_k(\vartheta)} p_j h_j \mathbf{s}_j \mathbf{s}_j^T + \sum_{l \notin g_k(\vartheta)} p_l h_l v_{li} \mathbf{s}_l \mathbf{s}_l^T + \sigma^2 \mathbf{I}, \\ \mathbf{c}_i &= \frac{\sqrt{p_i(n)}}{1 + p_i(n) \mathbf{s}_i^T \mathbf{A}_{ki}^{-1}(\mathbf{p}(n)) \mathbf{s}_i} \mathbf{A}_{ki}^{-1}(\mathbf{p}(n)) \mathbf{s}_i \end{aligned} \quad (19)$$

for the uplink, and

$$\begin{aligned} (\text{D-PC}) \quad \mathbf{A}_{ki}(\mathbf{p}(n)) &= \sum_{j \neq i, j \in g_k(\vartheta)} p_j h_i(\mathbf{s}_j^i) (\mathbf{s}_j^i)^T + \sum_{l \notin g_k(\vartheta)} p_l h_l v_{li}(\mathbf{s}_l^i) (\mathbf{s}_l^i)^T + \sigma^2 \mathbf{I}, \\ \mathbf{c}_i &= \frac{\sqrt{p_i(n)}}{1 + p_i(n) (\mathbf{s}_i^i)^T \mathbf{A}_{ki}^{-1}(\mathbf{p}(n)) (\mathbf{s}_i^i)} \mathbf{A}_{ki}^{-1}(\mathbf{p}(n)) (\mathbf{s}_i^i) \end{aligned} \quad (20)$$

for the downlink. The power for user i is then adjusted to meet the SIR constraint:

$$\mathbf{p}(n+1) = \mathbf{I}(\mathbf{p}(n)). \quad (21)$$

We should note that due to the presence of ISeCI, the iterative power control algorithms that are run in each sector for a given arrangement interact with each other. However, cell-wide convergence is guaranteed no matter in which order the sector power updates are executed—thanks to the asynchronous convergence theorem in [9]. We also note that the resulting MMSE filter suppresses both the intrasector interference and the ISeCI that each user experiences.

When the number of feasible sectorization arrangements is S_f , the jointly optimum sectorization arrangement, power control, and receiver filters are found by the following algorithm.

(1) For $l = 1, \dots, S_f$, for sectorization arrangement l , find the minimum total transmit power, TP_l , using the MMSE power control algorithm described above.

(2) Choose the sectorization arrangement that yields $\min_l TP_l$, along with the corresponding transmit power values and receiver filters found in step (1).

As explained before, the number of feasible sectorization arrangements $S_f \leq \binom{M}{K}$. Thus, the number of power control algorithms to be run is $O(KM^K)$. In practice, however, the number of feasible scenarios can be significantly smaller. We note that cells that are heavily loaded are the ones which would significantly benefit from employing several interference management techniques in a jointly optimum fashion. In such cases, it is unlikely that sectorization arrangements, where there is a small fraction of the sectors serving most of the users, would turn out to be infeasible; that is, not all users can achieve their target SIR. Also, physical constraints of the directional sector antennas typically impose a minimum angular separation constraint between users, in addition to minimum and maximum sector angle constraints. Nevertheless, when the number of users/sectors is relatively large, we may opt to look for solutions with reduced complexity that result in near-optimum performance. Such algorithms are presented next.

6. NEAR-OPTIMUM SECTORIZATION

6.1. Ignoring ISeCI

If the directional antenna patterns have a fast decay for the out-of-sector range, the amount of ISeCI experienced by a user would be small as compared to intrasector interference. In such cases, sectorizing the cell by ignoring the intersector interference is expected to perform close to the optimum.

Ignoring the existence of ISeCI leads to perfectly isolated sectors, as considered in [2]. In this case, as [2] shows, the sectorization problem can be converted to a shortest path problem on a network that is constructed from the string obtained from breaking the ring in Figure 1 between any two nodes. Such M shortest path problems should be solved, each of which has complexity $O(KM^2)$. The work in [12] showed that in the special case where equicorrelated signature sequences are used, a closed-form expression for sector

received power exists for UTP, and the weight of each edge of the network can be calculated readily. However, for arbitrary signature sequences, as we consider here, the calculation of each weight entails running the iterative power control algorithms, U-PC or D-PC. Thus, the sectorization complexity is reduced only when $K > 3$.

6.2. Variations on equal loading

An intuitively pleasing and simple solution is to design sectors such that an equal number of users reside in each sector. The intuition behind is to try to equalize the “load” per sector as much as possible. The angular boundaries of sectors are determined such that an equal number of users reside in each sector with respect to a reference point. Next, the corresponding transmit power values and receiver filters are found via running the power control algorithm described in Section 2. This process has to be repeated $\lceil M/K \rceil$ times by shifting the reference point with 0° angle to the next user from the previous reference point. The sectorization arrangement with minimum total transmit power is selected as the best “equal number of users per sector solution.”

When the terminal distribution is uniform, equal load-per-sector solution is expected to work well. However, as the terminal distribution becomes nonuniform, equal load-per-sector solution needs to be improved to achieve near-optimum performance. We have observed that the following algorithm improves the equal load-per-sector solution and works near optimum in a range of scenarios. Once the equal load-per-sector solution that yields the minimum (cell) total power is found, we move the boundaries of the sector with *the minimum total power* to include users from neighboring cells, in an effort to try to shift a user that may cause substantial increase in sector power to the neighboring sector that has the least power expenditure. Specifically, we try to maximize the minimum P_k , where P_k is the sector received power in the uplink case, or the sector transmit power in the downlink case for the k th sector antenna. Although it is difficult to draw general conclusions for a system with no particular channel or signature set structure, we find that running a couple of the above iteration improves the performance in all of our simulation scenarios considerably as compared to the equal number of users per sector performed near optimum.

7. NUMERICAL RESULTS

7.1. Perfect channel estimation

We consider a heavily loaded CDMA cell with processing gain $N = 16$ and number of users $M = 25$. We assume three paths for both uplink and downlink. In the multipath model, the delay of the first path is set to 0. For all other channel taps, each successive tap is delayed by either 1 or 2 chips, with probability 1/2, that is, the delay spread is at most 4 chips. The channel tap difference between two successive tap gains is $|A|$ dB, where $A \sim N(0, 20)$. The cell is to be partitioned to $K = 6$ sectors. In the antenna pattern model, we set $\theta_2 - \theta_1 = 15^\circ$, $P = -10$ dB, and the maximum angle constraint ($\max(2\theta_1) = 120^\circ$). We assume no

TABLE 1: Results for the system in Figure 4. Total transmit power is in watts.

Method	Total trans. power	Sector arrangement
Uplink with uplink OS	1.3107	1 7, 12, 16, 21, 23
Uplink with downlink OS	1.3239	1 7, 11, 15, 20, 22
Downlink with downlink OS	1.1781	1 7, 11, 15, 20, 22
Downlink with uplink OS	1.2143	1 7, 12, 15, 21, 23

TABLE 2: Results for the system in Figure 5.

Method	Total trans. power	Sector arrangement
Uplink with uplink OS	5.1570	3, 8, 12, 16, 21, 25
Uplink with downlink OS	5.8712	2, 5, 11, 15, 21, 25
Downlink with downlink OS	4.9123	2, 5, 11, 15, 21, 25
Downlink with uplink OS	5.2204	3, 8, 12, 16, 21, 25

channel estimation error in this section. AWGN variance is set to $\sigma^2 = 10^{-13}$, which is appropriate for 1 MHz channel bandwidth.

The numerical results demonstrate the performances of optimum sectorization (OS), sectorization done ignoring the ISeC as explained in Section 6.1 (NOS-1), and sectorization done using the algorithm described in Section 6.2 (NOS-2). To assess the benefit of adaptive uplink and downlink cell sectorizations with multiuser detection (receiver filter optimization), we compared our results with (i) conventional sectorization (equal angular partition) when the base station (for the uplink) or each terminal (for the downlink) employs MMSE multiuser detection (EAP), and (ii) adaptive optimum sectorization when the base station or each terminal uses adaptive matched filters (AMFs). For clarity of presentation of our results, we number all M users in the cell in the order of the increasing angular distances from a reference line. In the tables, we present that “the sector arrangement” identifies the users that belong to each sector. Among M users throughout the sectors, sector arrangement (A_1, A_2, \dots, A_K) corresponds to sector 1 which has users $(A_1, \dots, A_2 - 1)$, sector 2 which has users $(A_2, \dots, A_3 - 1)$, \dots , and sector K which has users $(A_K, \dots, M, 1, \dots, A_1 - 1)$. For example, among 25 users in a cell, sector arrangement $(1, 3, 7, 13, 19, 23)$ corresponds to sector 1 which has users 1 and 2, sector 2 which has users 3–6, sector 3 which has users 7–12, and so on.

Our first set of numerical results aims to show the difference between the optimum sectorization arrangements for uplink and downlink. Figures 4 and 5 show the optimum sectorization for uplink and downlink with random signatures and single path, for uniform and nonuniform user distributions over the cell. Tables 1 and 2 show the corresponding optimum total transmit power values. They also tabulate the resulting transmit powers for uplink when downlink OS arrangement is used, and for downlink when uplink OS arrangement is used. As expected, the optimum arrangements are different.

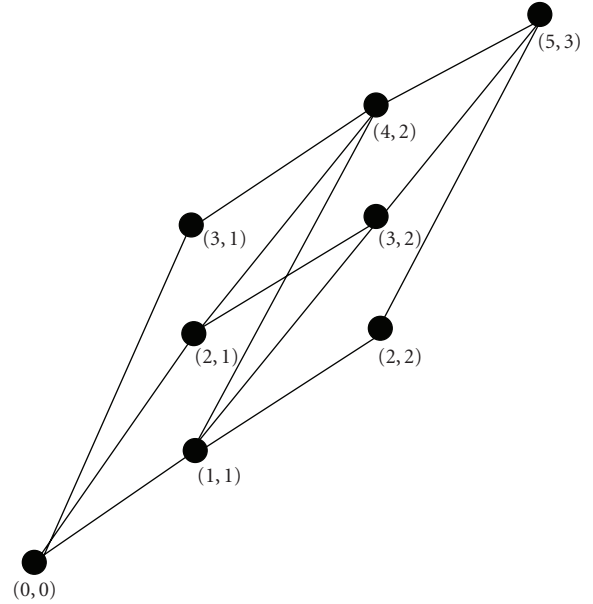


FIGURE 3: The network constructed for $M = 5$ users, and $K = 3$ sectors.

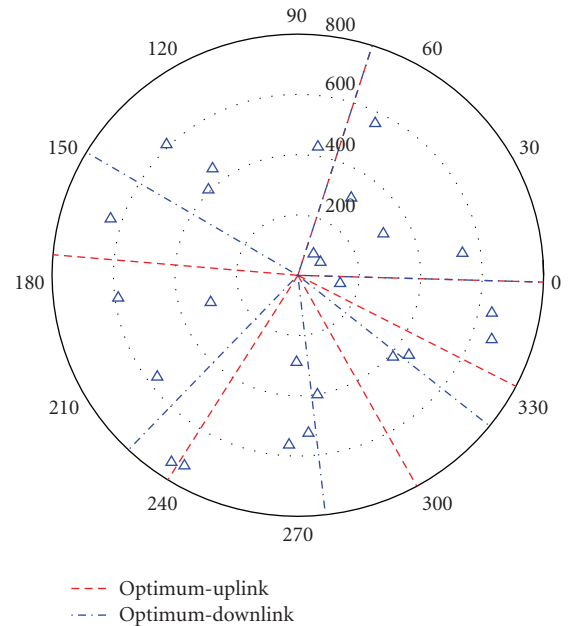


FIGURE 4: Comparison of optimum sectorization with random signature for uplink and downlink; uniform terminal distribution.

Figures 6, 7, 8, and 9 show uplink and downlink sector boundaries for uniform and nonuniform user distributions, respectively. Tables 3, 4, 5, and 6 show the total transmit powers and sectorization arrangements of the optimum sectorization (OS), NOS-1, and NOS-2 in uniform and nonuniform distributions, respectively. It is seen that the optimum as well as near-optimum algorithms we proposed outperform EAP and AMF; that is, employing all three interference management methods, power control, receiver filter

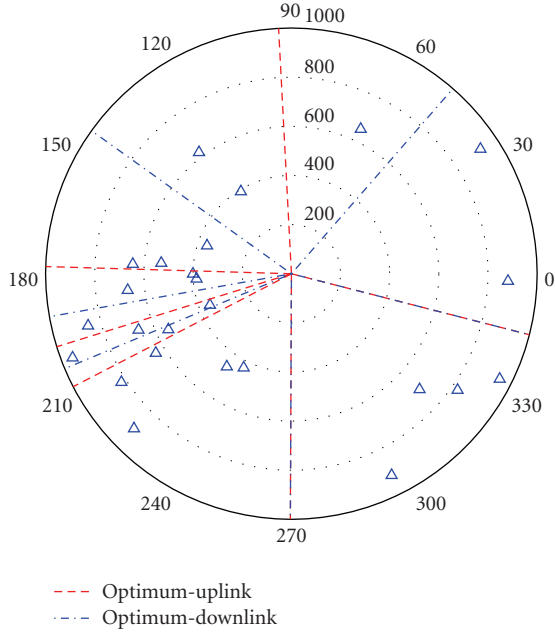


FIGURE 5: Comparison of optimum sectorization with random signature for uplink and downlink; nonuniform terminal distribution.

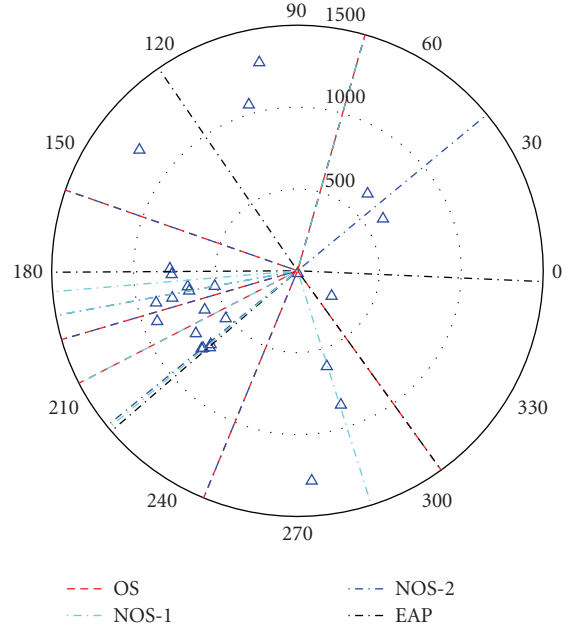


FIGURE 7: Sector boundaries for the uplink of a CDMA system with nonuniform user distribution. Number of users, $M = 25$; processing gain, $N = 16$; number of sectors, $K = 6$.

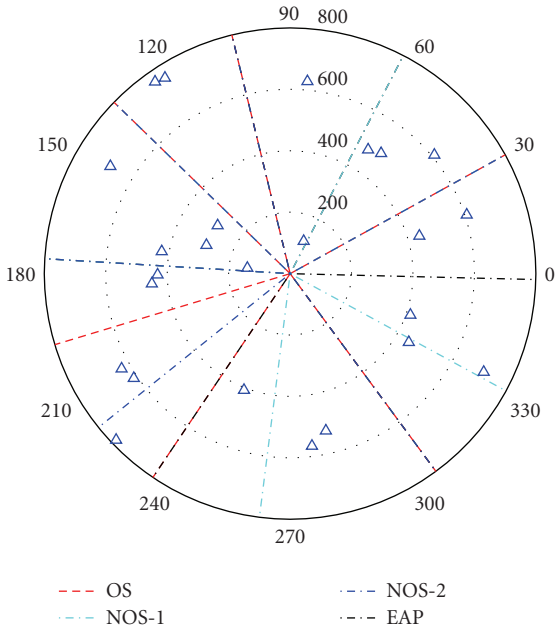


FIGURE 6: Sector boundaries for the uplink of a CDMA system with uniform user distribution. Number of users, $M = 25$; processing gain, $N = 16$; number of sectors, $K = 6$.

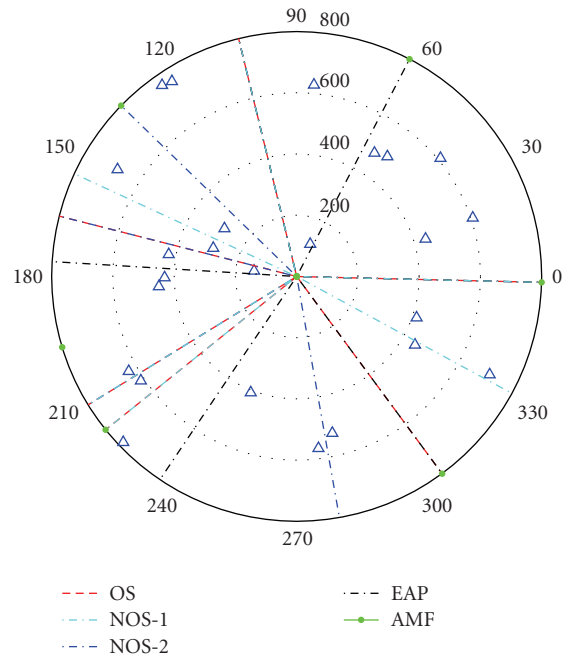


FIGURE 8: Sector boundaries for the downlink of a CDMA system with uniform user distribution. Number of users, $M = 25$; processing gain, $N = 16$; number of sectors, $K = 6$.

optimization, and adaptive sectorization jointly results in better performance than employing both power control and receiver optimization (EAP), and power control and adaptive sectorization with adaptive matched filters (AMFs). In fact, AMF [2] returns a feasible solution only for the downlink uniform distribution example. As expected, for uniform user distribution, the equal number of users per sector solu-

tion works well with the added advantage of MMSE receiver filters to suppress intra- and intersector interferences. However, for nonuniform user distribution, EAP has poor performance and requires about 3 dB more transmit power than OS for the uplink (see Table 4). Lastly, we note that NOS-2, the computationally simplest algorithm of the three algorithms we propose, generally performs near optimum and is

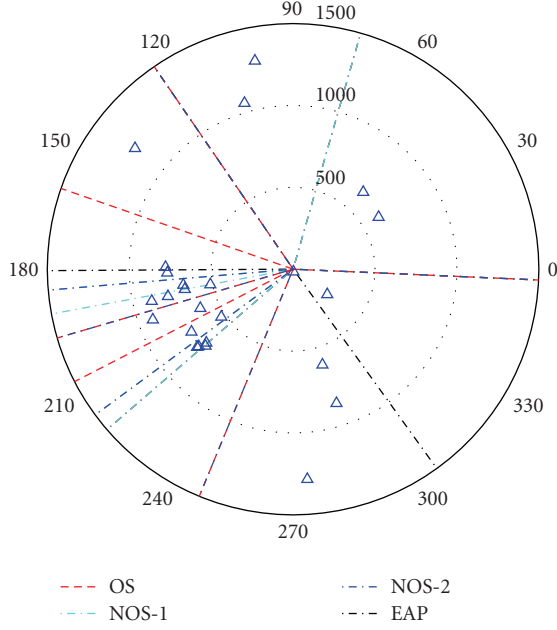


FIGURE 9: Sector boundaries for the downlink of a CDMA system with nonuniform user distribution. Number of users, $M = 25$; processing gain, $K = 6$; number of sectors, $K = 6$.

TABLE 3: Results for the system in Figure 6.

Method	Total trans. power	Sector arrangement
OS	1.7932	3, 8, 10, 17, 20, 23
NOS-1	2.131	3, 6, 10, 15, 21, 24
NOS-2	1.8634	3, 8, 10, 15, 19, 23
EAP	2.2554	1, 6, 8, 15, 20, 23
AMF		Infeasible

TABLE 4: Results for the system in Figure 7.

Method	Total trans. power	Sector arrangement
OS	9.1034	3, 6, 13, 15, 21, 25
NOS-1	12.4324	3, 8, 10, 15, 19, 24
NOS-2	10.5515	2, 6, 10, 13, 18, 21
EAP	20.6324	1, 3, 5, 7, 20, 25
AMF		Infeasible

better than NOS-1. NOS-1, which simply ignores the ISeCI, also has good performance, at the expense of computational complexity that may not be much lower than that of OS. The degree of suboptimality of NOS-1 is strictly a function of the antenna patterns; that is, the smaller the out-of-sector range of the directional antenna is (fast decay of side lobes), the closer NOS-1 will perform to OS.

7.2. Channel estimation error

The adaptive cell sectorization concept relies on the fact that users' channels/physical locations are known. Hence, it is appropriate to investigate the robustness of the methods against channel estimation errors. In this section, we provide numer-

TABLE 5: Results for the system in Figure 8.

Method	Total trans. power	Sector arrangement
OS	2.5114	1, 8, 13, 18, 19, 23
NOS-1	2.5457	1, 8, 12, 18, 19, 24
NOS-2	2.5300	1, 8, 10, 13, 18, 22
EAP	2.5977	1, 6, 8, 15, 20, 23
AMF	2.8262	1, 6, 10, 17, 19, 23

TABLE 6: Results for the system in Figure 9.

Method	Total trans. power	Sector arrangement
OS	10.8223	1, 5, 6, 13, 15, 21
NOS-1	11.7079	1, 3, 8, 10, 17, 20
NOS-2	10.9893	1, 5, 8, 13, 17, 21
EAP	13.7195	1, 3, 5, 7, 20, 25
AMF		Infeasible

TABLE 7: Total transmit power (TP) for uniform terminal distribution, $\gamma^* = 5$.

	σ_h^2	0.001	0.01	0.05	0.1	0.15
Uplink	$\bar{\gamma}$	5.4	5.8	6.6	7.2	7.8
	TP	1.9314	2.1063	2.5105	3.0644	4.5743
Downlink	$\bar{\gamma}$	5.2	5.8	6.4	7.0	7.4
	TP	2.6148	2.9510	3.4680	4.2674	5.2034

TABLE 8: Total transmit power (TP) for nonuniform terminal distribution, $\gamma^* = 5$.

	σ_h^2	0.001	0.01	0.05	0.1	0.15
Uplink	$\bar{\gamma}$	5.2	5.8	6.6	7.2	8.0
	TP	9.5024	10.7346	13.0244	16.3320	23.4525
Downlink	$\bar{\gamma}$	5.2	5.8	6.4	7.0	7.4
	TP	11.2585	12.6676	14.7034	17.7137	22.1825

ical results to show the robustness of optimum sectorization against Gaussian channel estimation errors. Estimated path loss gain \hat{h} is modeled as

$$\hat{h} = h + e; \quad \frac{E(\hat{h} - h)^2}{h^2} = \sigma_h^2, \quad (22)$$

where h is the true channel gain and $E(e) = 0$. Figures 10 and 11 show probability ($\text{SIR} > \gamma^*$) versus target SIR in MMSE power control for uplink and downlink, respectively. The target SIR (TSIR) in MMSE power control is the actual target SIR value used in the power control algorithms U-PC and D-PC, whereas γ^* is the minimum QoS requirement for reliable communication. In the presence of estimation errors, TSIR should be chosen such that the original target for reliable communication γ^* should be achieved most of the time. Hence, TSIR should include a margin to compensate for channel estimation errors. We set TSIR to the value that satisfies probability ($\text{SIR} > \gamma^*$) = 0.9 in Figures 9 and 10 and term it as *effective target* SIR, $\bar{\gamma}$. Tables 7 and 8 show the resulting total transmit power for different σ_h^2

TABLE 9: Robustness of optimum sectorization against Gaussian estimation error.

		σ_h^2	0.001	0.01	0.05	0.1	0.15
Uniform	Uplink	Robustness	85%	65%	54%	49%	46%
	Downlink	Robustness	99.9%	96%	63%	50%	44%
Nonuniform	Uplink	Robustness	99.9%	99.9%	94%	87%	82%
	Downlink	Robustness	99.9%	99%	90%	83%	72%

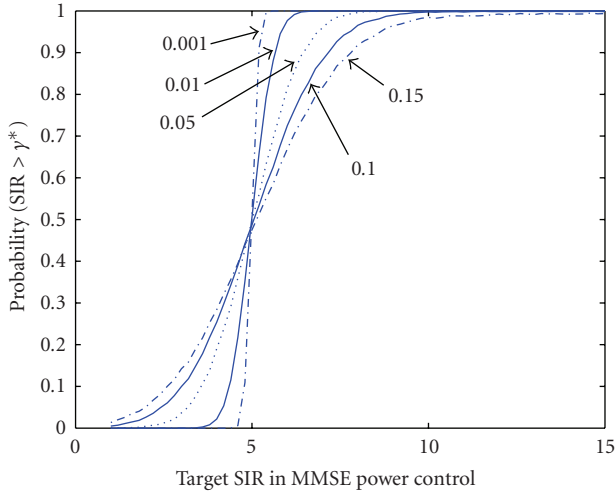


FIGURE 10: Uplink probability ($SIR > \gamma^*$) versus TSIR for Gaussian channel estimation error $\sigma_h^2 = 0.001, 0.01, 0.05, 0.1, 0.15, \gamma^* = 5$.

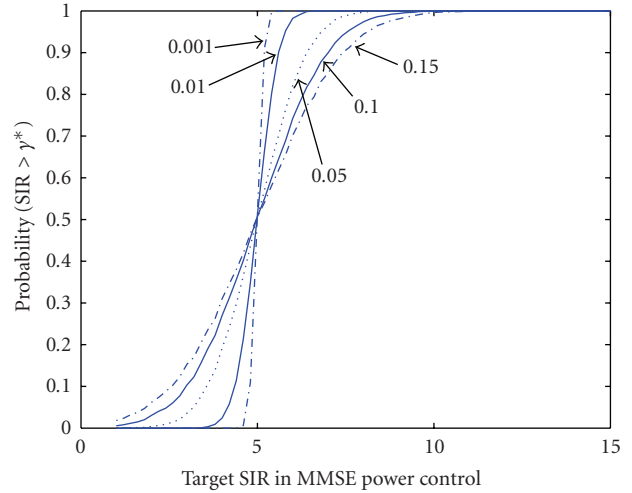


FIGURE 11: Downlink probability ($SIR > \gamma^*$) versus TSIR for Gaussian channel estimation error $\sigma_h^2 = 0.001, 0.01, 0.05, 0.1, 0.15, \gamma^* = 5$.

values. Figures 12 and 13 show the convergence of the SIR for each user for $\sigma_h^2 = 0.001$ and $\sigma_h^2 = 0.01$, respectively. As expected, increased normalized estimation error variance causes the total minimum transmit power to increase. Table 9 shows the robustness of optimum sectorization against Gaussian channel estimation error. The percentages shown represent the percentages of channel estimation error realizations that yield the same optimum adaptive cell sectorization arrangement as the ones that use the perfect channel estimates. For example, at $\sigma_h^2 = 0.01$ for nonuniform distribution, for 99.9% of the time, the optimum sectorization arrangement does not change. It is observed that the scenario with the uniform distribution of users is more vulnerable to estimation errors as compared to the nonuniform distribution. This may be attributed to the fact that when the users are uniformly distributed in the cell, the number of feasible sectorization arrangements is a lot higher than in the case of nonuniform distribution. However, note that in general the cases of nonuniform user distribution, which appears to be fairly robust to estimation errors, are of interest since adaptive sectorization is more beneficial in such scenarios.

8. CONCLUSION

In this paper, we considered the joint optimization problem of cell sectorization, transmit power control, and linear receiver filters and provided a comprehensive study for CDMA cells where the base station is equipped with variable beamwidth directional antennas, and the base station

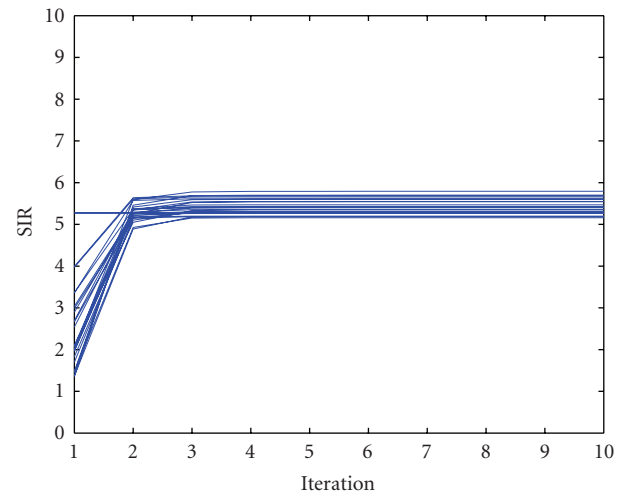


FIGURE 12: Uplink individual user SIR convergence for Gaussian channel estimation error $\sigma_h^2 = 0.001, \bar{\gamma} = 5.4$.

(for uplink) and the terminals (for downlink) have the ability to perform linear multiuser detection. We formulated the problems for uplink and downlink for arbitrary signature sequences and observed that in general the resulting sectorization arrangements that optimize the uplink user capacity would be different from those in the downlink. We proposed algorithms that would find the optimum solution, as well as near-optimum solutions with reduced complexity.

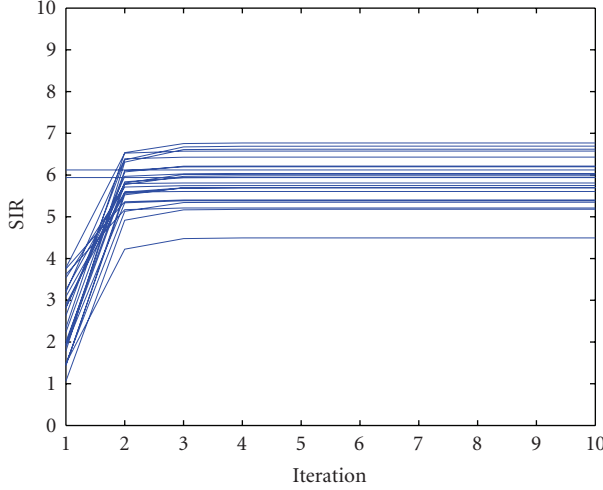


FIGURE 13: Uplink individual user SIR convergence for Gaussian channel estimation error $\sigma_h^2 = 0.01$, $\bar{\gamma} = 5.8$.

Numerical results confirm that intelligently combining power control, receiver filter design, and cell sectorization leads to improved uplink and downlink user capacities as compared to employing one or a couple of these interference management methods. That is, the cell can serve more simultaneous users with the same resources. We also numerically tested the robustness of cell sectorization arrangements against channel gain estimation errors and found that, for a range of scenarios of interest, the optimum sectorization arrangement stays the same, and we could compensate for channel estimation errors by a slight elevation in the total transmit power.

In conclusion, although exploring the interactions of the three interference management methods considered in this paper, power control, sectorization, and multiuser detection requires more complexity on system design as compared to an unoptimized system, the improvement in user capacity that is achieved may very well justify the additional complexity. This is true especially for slowly changing environments where channel gains and user activity status do not change frequently.

APPENDIX

A. PROOF OF OBSERVATION 1

Uplink transmit power is minimized when the SIR constraint in (12) is achieved with equality for all users, that is,

$$\begin{bmatrix} (\mathbf{s}_1^\top \mathbf{s}_1)^2 & -\gamma^* (\mathbf{s}_1^\top \mathbf{s}_2)^2 & \cdot & -\gamma^* (\mathbf{s}_1^\top \mathbf{s}_M)^2 \\ -\gamma^* (\mathbf{s}_2^\top \mathbf{s}_1)^2 & (\mathbf{s}_2^\top \mathbf{s}_2)^2 & \cdot & -\gamma^* (\mathbf{s}_2^\top \mathbf{s}_M)^2 \\ \cdot & \cdot & \cdot & \cdot \\ -\gamma^* (\mathbf{s}_M^\top \mathbf{s}_1)^2 & -\gamma^* (\mathbf{s}_M^\top \mathbf{s}_2)^2 & \cdot & (\mathbf{s}_M^\top \mathbf{s}_M)^2 \end{bmatrix} \begin{bmatrix} p_1 h_1 \\ p_2 h_2 \\ \cdot \\ p_M h_M \end{bmatrix} = \begin{bmatrix} \gamma^* \sigma^2 (\mathbf{s}_1^\top \mathbf{s}_1) \\ \gamma^* \sigma^2 (\mathbf{s}_2^\top \mathbf{s}_2) \\ \cdot \\ \gamma^* \sigma^2 (\mathbf{s}_M^\top \mathbf{s}_M) \end{bmatrix}. \quad (\text{A.1})$$

Equation (A.1) has the form

$$[\mathbf{I} - \gamma^* \mathbf{F}] \mathbf{p}_r = \gamma^* \sigma^2 \mathbf{1}, \quad (\text{A.2})$$

where $\mathbf{p}_r = [p_1 h_1, p_2 h_2, \dots, p_M h_M]^\top$ is the uplink received power vector. Note that $\mathbf{s}_i^\top \mathbf{s}_i = 1$ due to the assumption of unit energy signatures. \mathbf{F} is the squared cross-correlation matrix whose diagonal entries are zeros. A nonnegative solution \mathbf{p}_r exists if and only if the Perron-Frobenius eigenvalue of \mathbf{F} is less than $1/\gamma^*$ [22]. The solution is

$$\mathbf{p}_r = \gamma^* \sigma^2 [\mathbf{I} - \gamma^* \mathbf{F}]^{-1} \mathbf{1} = \gamma^* \sigma^2 \mathbf{A} \mathbf{1}. \quad (\text{A.3})$$

Observe that since \mathbf{F} is symmetric, \mathbf{A} is symmetric, that is, $A_{ij} = A_{ji}$. The optimum transmit power value for user i is

$$p_i = \frac{\gamma^* \sigma^2}{h_i} \sum_j A_{ij}, \quad i = 1, \dots, M \quad (\text{A.4})$$

and the total minimum sector transmit power is

$$\sum_i p_i = \gamma^* \sigma^2 \sum_i \frac{1}{h_i} \sum_j A_{ij}, \quad i, j = 1, \dots, M. \quad (\text{A.5})$$

For the downlink, we also have to satisfy all SIR constraints with equality leading to the matrix equation

$$\begin{bmatrix} (\mathbf{s}_1^\top \mathbf{s}_1)^2 & -\gamma^* (\mathbf{s}_1^\top \mathbf{s}_2)^2 & \cdot & -\gamma^* (\mathbf{s}_1^\top \mathbf{s}_M)^2 \\ -\gamma^* (\mathbf{s}_2^\top \mathbf{s}_1)^2 & (\mathbf{s}_2^\top \mathbf{s}_2)^2 & \cdot & -\gamma^* (\mathbf{s}_2^\top \mathbf{s}_M)^2 \\ \cdot & \cdot & \cdot & \cdot \\ -\gamma^* (\mathbf{s}_M^\top \mathbf{s}_1)^2 & -\gamma^* (\mathbf{s}_M^\top \mathbf{s}_2)^2 & \cdot & (\mathbf{s}_M^\top \mathbf{s}_M)^2 \end{bmatrix} \begin{bmatrix} q_1 \\ q_2 \\ \cdot \\ q_M \end{bmatrix} = \begin{bmatrix} \frac{\gamma^* \sigma^2 (\mathbf{s}_1^\top \mathbf{s}_1)}{h_1} \\ \frac{\gamma^* \sigma^2 (\mathbf{s}_2^\top \mathbf{s}_2)}{h_2} \\ \cdot \\ \frac{\gamma^* \sigma^2 (\mathbf{s}_M^\top \mathbf{s}_M)}{h_M} \end{bmatrix}. \quad (\text{A.6})$$

Defining $\mathbf{u} = [1/h_1, 1/h_2, \dots, 1/h_M]^\top$, the solution for the optimum downlink powers is

$$\mathbf{q} = \gamma^* \sigma^2 [\mathbf{I} - \gamma^* \mathbf{F}]^{-1} \mathbf{u} = \gamma^* \sigma^2 \mathbf{A} \mathbf{u}. \quad (\text{A.7})$$

The downlink transmit power for user i is

$$q_i = \gamma^* \sigma^2 \sum_j \frac{A_{ij}}{h_j}. \quad (\text{A.8})$$

The total minimum downlink sector power is

$$\sum_i q_i = \gamma^* \sigma^2 \sum_i \sum_j \frac{A_{ij}}{h_j} = \gamma^* \sigma^2 \sum_j \frac{1}{h_j} \sum_i A_{ij}. \quad (\text{A.9})$$

Therefore,

$$\sum_i p_i = \sum_i q_i \quad (\text{A.10})$$

because $A_{ij} = A_{ji}$.

REFERENCES

- [1] F. Adachi, M. Sawahashi, and H. Suda, "Wideband DS-CDMA for next-generation mobile communications systems," *IEEE Communications Magazine*, vol. 36, no. 9, pp. 56–69, 1998.
- [2] C. U. Saraydar and A. Yener, "Adaptive cell sectorization for CDMA systems," *IEEE Journal on Selected Areas in Communications*, vol. 19, no. 6, pp. 1041–1051, 2001.
- [3] A. Yener, R. D. Yates, and S. Ulukus, "Interference management for CDMA systems through power control, multiuser detection, and beamforming," *IEEE Transactions on Communications*, vol. 49, no. 7, pp. 1227–1239, 2001.
- [4] J. Zander, "Performance of optimum transmitter power control in cellular radio systems," *IEEE Transactions on Vehicular Technology*, vol. 41, no. 1, pp. 57–62, 1992.
- [5] R. Lupas and S. Verdu, "Linear multiuser detectors for synchronous code-division multiple access channels," *IEEE Transactions on Information Theory*, vol. 35, no. 1, pp. 123–136, 1989.
- [6] U. Madhow and M. L. Honig, "MMSE interference suppression for direct-sequence spread-spectrum CDMA," *IEEE Transactions on Communications*, vol. 42, no. 12, pp. 3178–3188, 1994.
- [7] S. Ulukus and R. Yates, "Adaptive power control and MMSE interference suppression," *Wireless Networks*, vol. 4, no. 6, pp. 489–496, 1998.
- [8] G. J. Foschini and Z. Miljanic, "A simple distributed autonomous power control algorithm and its convergence," *IEEE Transactions on Vehicular Technology*, vol. 42, no. 4, pp. 641–646, 1993.
- [9] R. D. Yates, "A framework for uplink power control in cellular radio systems," *IEEE Journal on Selected Areas in Communications*, vol. 13, no. 7, pp. 1341–1347, 1995.
- [10] S. Verdu, *Multiuser Detection*, Cambridge University Press, Cambridge, UK, 1998.
- [11] J. C. Liberti and T. S. Rappaport, *Smart Antennas for Wireless Communications: Is-95 and Third Generation Cdma Applications*, Prentice-Hall, Upper Saddle River, NJ, USA, 1999.
- [12] C. Oh and A. Yener, "Adaptive CDMA cell sectorization with linear multiuser detection," in *Proceedings of the 58th IEEE Vehicular Technology Conference (VTC '03)*, vol. 2, pp. 962–966, Orlando, Fla, USA, October 2003.
- [13] R. Giuliano, F. Mazzenga, and F. Vatalaro, "Adaptive cell sectorization for UMTS third generation CDMA systems," in *Proceedings of the 53rd IEEE Vehicular Technology Conference (VTC '01)*, vol. 1, pp. 219–223, Rhodes, Greece, May 2001.
- [14] J. Zhang, J. Liu, Q. Zhang, W. Zhu, B. Li, and Y.-Q. Zhang, "An efficient algorithm for adaptive cell sectoring in CDMA systems," in *Proceedings of IEEE International Conference on Communications (ICC '03)*, vol. 2, pp. 1238–1242, Anchorage, Alaska, USA, May 2003.
- [15] A. Sabharwal, D. Avidor, and L. Potter, "Sector beam synthesis for cellular systems using phased antenna arrays," *IEEE Transactions on Vehicular Technology*, vol. 49, no. 5, pp. 1784–1792, 2000.
- [16] J. E. Smee and H. C. Huang, "Mitigating interference in wireless local loop DS-CDMA systems," in *Proceedings of the 9th IEEE International Symposium on Personal, Indoor and Mobile Radio Communications (PIMRC '98)*, vol. 1, pp. 1–5, Boston, Mass, USA, September 1998.
- [17] M. K. Karakayali, R. Yates, and L. Razoumov, "Joint power and rate control in multiaccess systems with multirate services," in *Proceedings of Conference on Information Sciences and Systems (CISS '03)*, Baltimore, Md, USA, March 2003.
- [18] R. W. Nettleton and W. Alavi, "Power control for a spread spectrum cellular mobile radio system," in *Proceedings of the 33rd IEEE Vehicular Technology Conference (VTC '83)*, pp. 242–246, Toronto, Canada, May 1983.
- [19] F. Rashid-Farrokhi, K. J. R. Liu, and L. Tassiulas, "Downlink power control and base station assignment," *IEEE Communications Letters*, vol. 1, no. 4, pp. 102–104, 1997.
- [20] R. D. Yates and C.-Y. Huang, "Integrated power control and base station assignment," *IEEE Transactions on Vehicular Technology*, vol. 44, no. 3, pp. 638–644, 1995.
- [21] M. R. Garey and D. S. Johnson, *Computers and Intractability: A Guide to the Theory of NP-Completeness*, W. H. Freeman, New York, NY, USA, 1991.
- [22] G. Alexander, *Nonnegative Matrices and Applicable Topics in Linear Algebra*, Ellis Horwood, Chichester, UK, 1987.